

9B.6 STATISTICAL ANALYSIS OF ORGANIZED CLOUD CLUSTERS ON WESTERN NORTH PACIFIC AND THEIR WARM CORE STRUCTURE

Kotaro Bessho*¹, Nakazawa Tetsuo¹, Shuji Nishimura², Koji Kato² and Shunsuke Hoshino¹

¹ Meteorological Research Institute, Tsukuba, Japan

² Japan Meteorological Agency / Meteorological Satellite Center, Kiyose, Japan

1. INTRODUCTION

There are many cloud clusters on tropical ocean of western North Pacific. Some clusters develop into tropical storms, but most of them disappear without developing into the storms. It is very important to distinguish the clusters, which become tropical storms or not. Operationally the Dvorak technique has been used widely to estimate the possibility of clusters to develop into tropical storms (Dvorak, 1975 and Dvorak, 1984). The Dvorak technique is a subjective analysis, and is used as a tool for judging a generation of tropical cyclones and evaluating the intensity of the cyclones such as central surface pressure and maximum wind speed from the features of cloud clusters and tropical cyclones observed by visible and infrared imagers. The index called as T-number is defined in Dvorak technique to express the intensity of tropical cyclone.

On the other hand, there is an improvement and enhancement of microwave sensors on board low orbital satellites. By using the results of the observation of those microwave sensors, there is a possibility to complement the Dvorak technique and judge the genesis of tropical cyclones objectively.

In this study, the status of largely Organized Cloud Clusters (OCCs), which include the OCCs Developing into tropical storms (DOCCs) and not developing into tropical storms (NOCCs), were investigated statistically. And on the basis of the statistical results, the differences between structures and developing processes of DOCC and NOCC were also examined with the data from microwave sensors especially of Advanced Microwave Sounding Unit (AMSU).

2. EARLY STAGE DVORAK ANALYSIS

As an Early stage Dvorak Analysis (EDA), Meteorological Satellite Center (MSC) of Japanese Meteorological Agency (JMA) has routinely watched OCC on western North Pacific with the possibility to develop into tropical storms which are defined in terms of Tsuchiya *et al.* (2001), and logged their locations and T-numbers from 1999.

The tropical cyclones is classified by JMA into four grades depending on Maximum Wind Speed (MWS) such as Typhoon (TY, MWS is more than 64 kt), Severe Tropical Storm (STS, MWS is more than 48 kt and less than 64 kt), Tropical Storm (TS, MWS is more than 34 kt and less than 48 kt), and

Tropical Depression (TD, MWS is less than 34 kt). Tropical cyclones, which have MWS more than 34 kt, are named by JMA and gale warnings are issued. EDA, which is employed to distinguish TD and TS, includes the next two steps.

As a first step, Cloud System Center (CSC) of cloud cluster is investigated. OCC is defined as the cloud cluster with CSC. CSC has the features as below which follow Dvorak (1984) (Figure 1). To determine the CSC, analysts in MSC select the finest character from these four cloud patterns.

- i) Dense and cold (-31°C or colder) overcast bands that show some curvature around a relatively warm area. They should curve at least one-fifth the distance around a ten degrees log spiral. When visible observations are available, cirrus will indicate anticyclone shear across the expected CSC.
- ii) Curved cirrus lines indicating a center of curvature within or near a dense, cold (-31°C or colder) overcast.
- iii) Curved low cloud lines showing a center of curvature within two degrees of a cold (-31°C or colder) cloud mass.
- iv) Cumulonimbus (Cb) clusters rotating cyclonically on animated images.

After detecting the CSC, T-number 1 (T1) diagnosis is started to judge the cyclogenesis as a second step of EDA. In this diagnosis T-number is regarded as one when cloud systems has all five conditions as below (Figure 2).

- 1: The cloud clusters have persisted for 12 hours or more.
- 2: The accuracy of estimation of CSC in the clusters is 2.5° latitude or less.
- 3: The CSC has persisted for 6 hours.
- 4: The clusters have dense, cold (-31°C or colder) overcasts that appear less than 2° latitude from CSC.
- 5: The extent of the overcasts is more than 1.5° latitude.

When T number becomes one or more, OCC is identified as TD (not yet TS). And when the MWS of TD has reached to 34 kt or more, OCC is judged as TS. OCC, whose T number is less than one, is called as Low pressure area (L) in EDA.

3. STATISTICAL ANALYSIS OF OCC

In this study, using the results of EDA, DOCC and NOCC were statistically analyzed, and their frequency and geographical locations of genesis, their duration, and so on were investigated.

For example, in EDA file 2004, there were 100 of OCCs on western North Pacific ocean. Among them, the number of

*Corresponding author address: Kotaro Bessho, Meteorological Research Institute, Tsukuba, Japan, 305-0052; e-mail: kbessho@mri-jma.go.jp

OCCs that developed into TS is 29. The number of OCCs, which developed into TD but not reached to TS, is 13. The remains that stayed on the stage of L is up to 58. In other words, almost 40 % of OCCs developing into TD, and 30% of OCCs finally became TS. The number of OCCs that developed into TD but not developed into TS is less than half number of OCCs into TS. Figure 3 shows the frequencies of occurrence of OCCs that reached to each developing stages. From this figure, it is found that the numbers of genesis of all OCCs and OCCs developing into TS (DOCC) are largest on August, and it means convection and organization of clouds were active in this month. The largest number of occurrence of OCCs that remained at L is seen in October.

To understand the geographical distributions of OCCs, western North Pacific ocean was divided into five regions following Zehr (1992). Figure 4 shows the percentage of occurrence of all OCCs in each region, 2004. From this figure, 58 % of all OCCs were included between 5° N and 20° N in latitude, and 125° E and 160° E in longitude, which is called as the primary genesis region in Zehr (1992). In the same region, the percentages of OCCs staying at, or developing into L, TD and TS are 52, 62 and 69 (not shown). Similar to Zehr (1992), the percentages of each OCC in the primary genesis region are almost 60.

For TS, the average periods from the detection of OCC to the judgment of TS are 50.5 hours in 2004. It means that OCC needs approximately two days to become TS. And averagely 18.6 hours are needed for TS to reach first time at the T-number 1 from its appearance as OCC. Meanwhile, durations of L from the detection as OCC to the disappearance are averagely only 8.0 hours.

4. WARM CORE STRUCTURE OF OCC ESTIMATED FROM AMSU

To investigate the inner structure of OCCs, air temperature profiles in OCCs were retrieved from AMSU brightness temperature data by using the DDK algorithm (Demuth *et al.* 2004 and Bessho *et al.* 2006). 100 cases of OCCs in 2004 were explored, and finally pressure - time cross sections of the air temperature anomalies in CSC of OCCs were drawn in 94 cases. To calculate the temperature anomalies, mean air temperature in the rectangle of 24° latitude X 24° longitude centered on the position of OCC at each pressure level was subtracted from the air temperature. And to draw the pressure - time cross sections, the temperature anomalies were also averaged at the rectangle of 4° latitude X 4° longitude centered on the position of OCC.

For example, Figure 5 shows the cross sections of two OCCs. One is numbered as 0455 (hereafter EDA0455), and the other is as 0457 (EDA0457). EDA0455 was first detected as OCC at 00z 17 Aug. 2004 on 10.4° N and 147.9° E. It reached to T-number 1 at 00z 18 Aug. on 10.5° N and 143.1°

E and became TD. And finally EDA0455 developed into TS at 00z 20 Aug. on 14.3° N and 136.0° E and was named as Aere (TS number is 0417 in JMA). So EDA0455 is one of DOCCs. On the other hands, EDA0457 was found as OCC at 06z 25 Aug. 2004 on 13.5° N and 153.0° E and 6hours later it became TD at almost same point. EDA0457 kept the status 24 hours, but at 12z 26 Aug. its CSC was lost and EDA0457 disappeared. So EDA0457 is one of NOCC.

From Fig. 5(a), it is found that positive temperature anomalies are located at the upper levels of 200 - 300 hPa. These positive anomalies show warm core structures of EDA0455. In this DOCC case, after reaching to the stage of TD, positive temperature anomalies were more than 1 K. At lower levels, the negative temperature anomalies are also shown. These are not reliable because the raw brightness temperature data were contaminated by heavy precipitation.

In the case of NOCC of EDA0457, negative temperature anomalies are seen at the upper levels from Fig. 5(b). This is an extreme case and most of NOCCs have positive temperature anomalies at upper levels. But those positive anomalies are usually less than 1 K in the cross sections.

Figure 6 includes horizontal snapshots of EDA0455 and EDA0457. They consisted of the image of air temperature anomalies at the level of 250 hPa retrieved from AMSU, almost simultaneously observed Tropical Rainfall Measuring Mission (TRMM) Microwave Imager (TMI) images, and Geostationary Operational Environmental Satellite - 9 (GOES -9) infrared image. TMI images are divided into Polarized Corrected Temperature (PCT) image based on the difference of brightness temperature between vertical and horizontal polarized 85 GHz (Spencer *et al.* 1989), and the raw brightness temperature image of 10 GHz. PCT is sensitive to ice crystals in high clouds and deep convections appears in the region of cold temperatures. And 10 GHz is also keen to rain drops at low altitude and heavy precipitations were expressed by warm temperatures.

From Fig. 6(a), EDA0455 is shown as low brightness temperature pattern, which is well organized, in GOES-9 infrared image. In TMI images, deep convections are identified near the center of OCC. It is also found that large positive anomalies are located in the region corresponded to the active convections. In the case of EDA0457, there is low brightness temperature area in GOES-9 image, which is a little bit smaller than that of EDA0455. And according to both images of TMI, EDA0457 has convective regions comparable with those of EDA0455. But in the image of AMSU temperature anomalies, negative region is found in the center of it. Convective regions on northwestern side of the EDA0457 images belonged to another cyclone. Warm core structures in tropical cyclones are considered as the results of active convections. EDA0457 has also deep convective systems, but no warm core. This discrepancy will be explained by further study.

In 94 cases of OCCs that were analyzed by pressure - time cross sections of air temperature anomalies, 28 cases of OCCs developing into TS. And 12 cases of OCCs also reached up to TD. OCCs staying at L are 54 cases. In this study, temperature anomalies more than 1 K are used as a threshold expressing obvious warm core structure. 26 cases of OCCs developing into TS have warm core structures. Also there are 6 cases of OCCs up to TD and 15 cases of OCCs staying at L, which have warm core structures. From these numbers, it is found that most of OCCs developing into TS have warm cores, and almost 70 % of OCCs staying at L have no warm cores. For 26 cases of OCCs developing into TS that have warm core structures, the average periods from the detection as OCC to the time at which the temperature anomalies more than 1 K are first recognized in cross sections are 18.5 hours. These durations are corresponds to the periods from appearance of OCC to first judgment of T1. And the average periods from the detection of OCC to the judgment of TS were 50.5 hours. It means statistically that for OCCs developing into TS, warm core structures were observed by AMSU before 32 hours until reaching to the stage of TS. On the other hand, for 15 cases of OCC staying at L that have warm core structure, the average periods from the detection of OCC to the first recognition of the temperature anomalies more than 1 K are only 5.6 hours. These short durations are depends on the short lifetime of OCCs staying at L.

From these statistical results, it is understood that there are large possibilities to detect and forecast the generation of TS by using the information of positive temperature anomalies at upper levels retrieved from AMSU observations.

REFERENCES:

- Bessho, K., M. DeMaria and J. A. Knaff, 2006: Tropical cyclone wind retrievals from the Advanced Microwave Sounding Unit (AMSU): application to surface wind analysis. *J. Appl. Meteor.*, (in printing).
- Demuth, J. L., M. DeMaria, J. A. Knaff and T. H. Vonder Haar, 2004: Evaluation of Advanced Microwave Sounding Unit tropical-cyclone intensity and size estimation algorithms. *J. Appl. Meteor.*, **43**, 282-296.
- Dvorak, V. F., 1975: Tropical cyclone intensity analysis and forecasting from satellite imagery. *Mon. Wea. Rev.*, **103**, 420-430.
- Dvorak, V. F., 1984: Tropical cyclone intensity analysis using satellite data. *NOAA Tech. Rep. NESDIS 11*, Washington, DC, 47pp.
- Spencer, R. W., H. M. Goodman, and R. E. Hood, 1989: Precipitation retrieval over land and ocean with SSM/I: Identification and characteristics of the scattering signal. *J. Atmos. Ocean. Technol.*, **6**, 254-273.

Tsuchiya, A., T. Mikawa and A. Kikuchi, 2001: Method of distinguishing between early stage cloud systems that develop into tropical storms and ones that do not. *Geophys. Mag. Series 2*, **4**, 49-59.

Zehr, R. M., 1992: Tropical cyclogenesis in the Western North Pacific. *NOAA Tech. Rep. NESDIS 61*, Washington, DC, 181 pp.

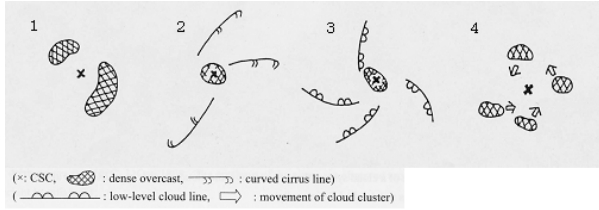


Figure 1. CSCs defined from four cloud patterns (i - iv). (after Tsuchiya *et al.* (2001))

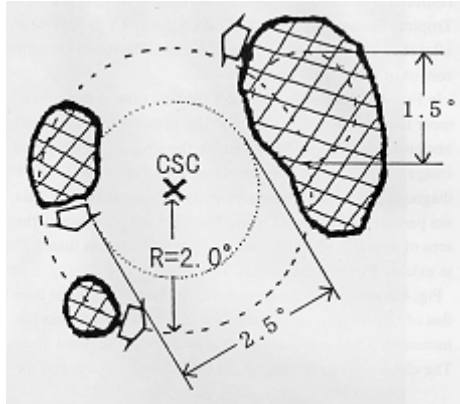


Figure 2. A conceptual model of the cloud clusters satisfying T1. The shaded areas are dense, cold (-31°C or colder) overcasts. The accuracy of estimation of CSC is expressed by the dotted circle around the CSC with a diameter of 2.5° (2:). The dashed circle with a radius of 2.0° indicates the region including the dense, cold overcasts (4:). The diameter of a circle drawn in the overcast on the right side of the CSC is 1.5° . This circle shows the size of the overcast (5:). (after Tsuchiya *et al.* (2001))

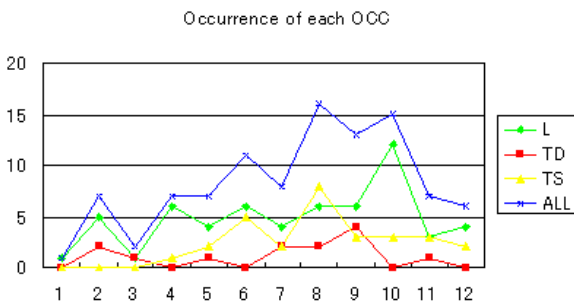


Figure 3. Frequencies of occurrence of OCCs that reached to each developing stages on each month in 2004.

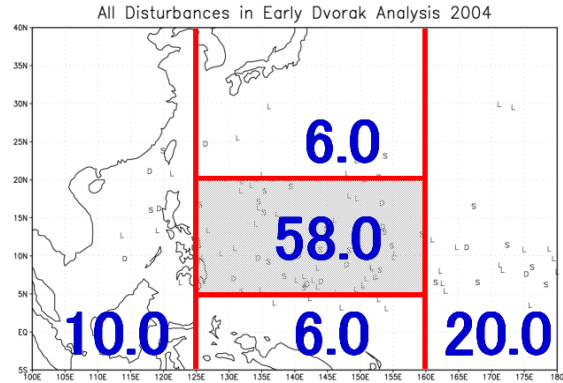


Figure 4. Percentages of occurrence of all OCCs in western North Pacific divided into five regions in 2004. Shaded area is primary genesis region in Zehr (1992).

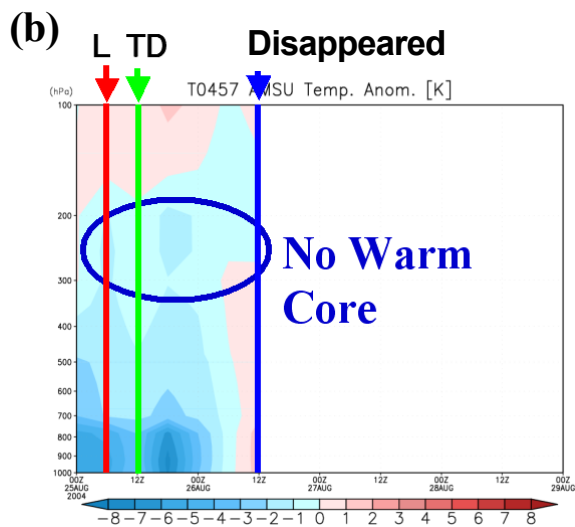
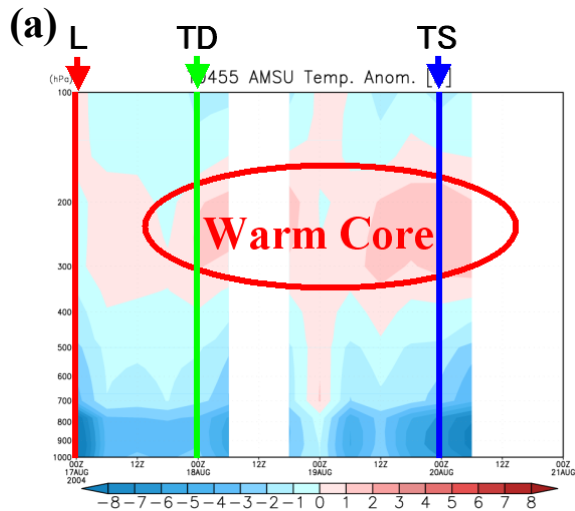


Figure 5. Pressure - time cross sections of air temperature anomalies retrieved from AMSU observations in the cases of EDA0455 (a) and EDA0457 (b).

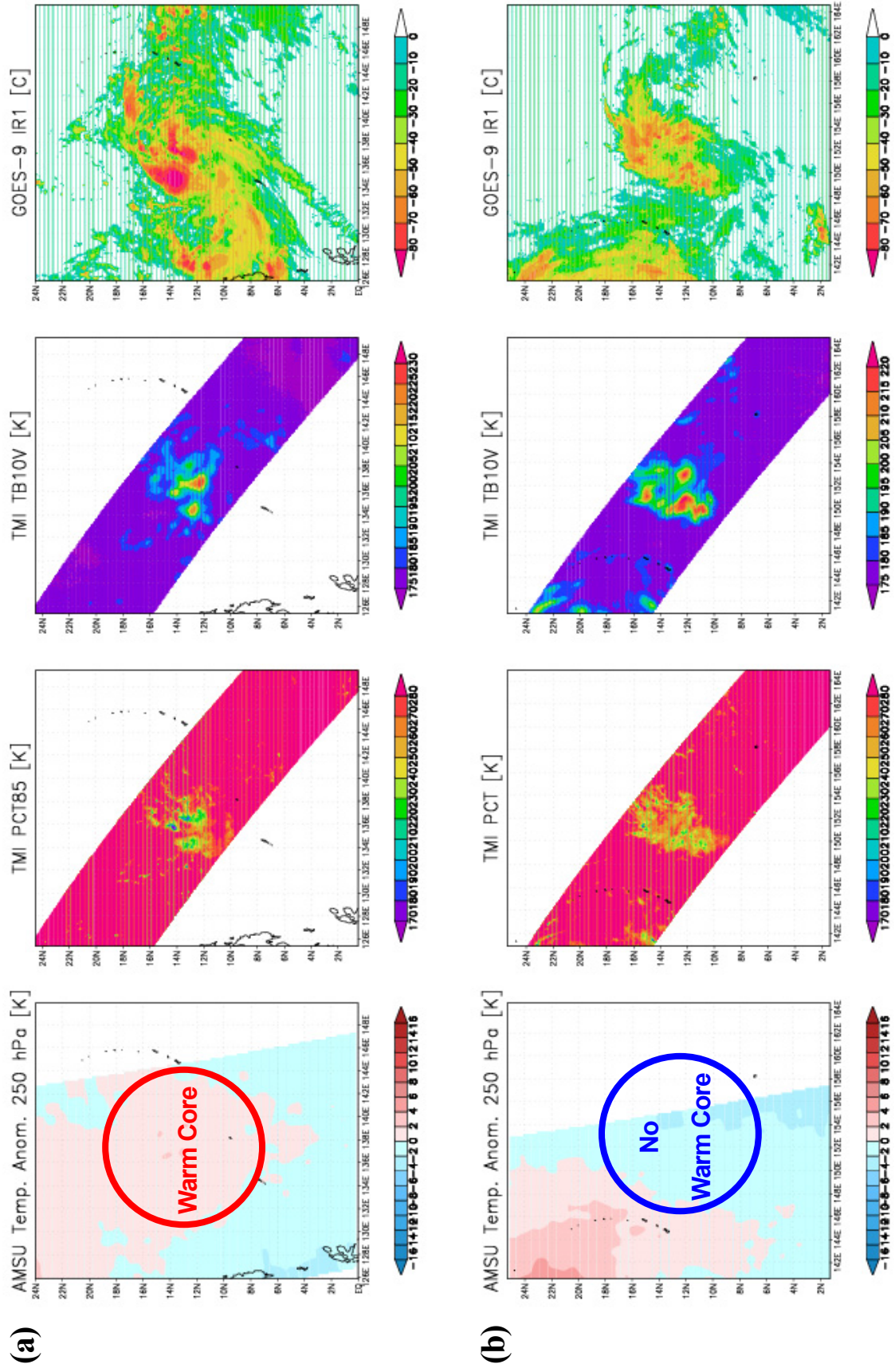


Figure 6. (a) Horizontal images of AMSU retrieved temperature anomalies at 250 hPa observed at 09:19z 19 Aug. 2004, TMI PCT derived from 85 GHz observed at 11:32z, TMI 10 GHz brightness temperatures and GOES-9 infrared brightness temperatures observed at 09:30z for EDA0455. (b) Same as (a) except for AMSU observation time at 08:37z 25 Aug. 2004, TMI at 07:40z and GOES-9 at 08:30z.